Transport and Structural Studies of Sulfonated Styrene−Ethylene Copolymer Membranes

J. M. Serpico,[†] S. G. Ehrenberg,[†] J. J. Fontanella,[‡] X. Jiao,[§] D. Perahia,*[,§] K. A. McGrady,[⊥] E. H. Sanders,[⊥] G. E. Kellogg,[#] and G. E. Wnek*[,⊥]

Dais Analytic Corporation, 11552 Prosperous Drive, Odessa, Florida 33556; Physics Department, U.S. Naval Academy, Annapolis, Maryland 21402-5026; Department of Chemistry, Clemson University, Clemson, South Carolina 29634-0973; Department of Chemical Engineering, Virginia Commonwealth University, Richmond, Virginia, 23284-3028; and Department of Medicinal Chemistry, Virginia Commonwealth University, Richmond, Virginia 23298-0540

Received February 15, 2002; Revised Manuscript Received May 13, 2002

ABSTRACT: The structure and proton conductivity of sulfonated styrene−ethylene copolymers have been studied. Conductivities in excess of 0.1 S/cm are obtained depending upon copolymer composition and sulfonation level. The dependence of conductivity on humidity has been measured and compared with that of Nafion and a partially sulfonated block copolymer. X-ray and neutron scattering studies suggest the presence of a bicontinuous network of hydrophilic and hydrophobic domains in water-swollen samples.

Introduction

Ionomers are polymers typically consisting of a hydrophobic backbone and hydrophilic, ionizable side chains. Ionomers bearing acidic groups are of great interest as proton-conducting membranes, frequently referred to as proton exchange membranes, or PEMs, for fuel cell applications. In a PEM fuel cell, the electrochemical reactions take place at the polymer−catalyst interface, and the polymeric membrane facilitates proton transfer across the membrane.[1] Key requirements for commercially viable PEMs are high proton conductivity, low gas transport rates, good mechanical stability, and low cost. Most polymers forming PEMs are essentially hydrogels, possessing remarkable water uptake capacities. In these systems, water molecules dissociate acid functionality and facilitate proton transport. Structure, dynamics, and transport measurements have been carried out on a variety of ion-containing polymers including perfluorinated ionomers such as Nafion (Figure 1a) and hydrocarbon-based systems such as styrene/ethylene−butylene/styrene (S-SEBS) triblock copolymer (Figure 1b).

In most bulk dry ionomers the ionic groups associate to form clusters, which expand after swelling of the polymer in polar solvents.[1−15] The shape and size of these clusters and their role in ion transport within their networks have been the focus of numerous studies.[1−12] In a recent spin probe microscopy study of dry ionomer films, ionic clusters have been directly observed.[6,9] On the basis of extensive neutron and X-ray studies, Gebel[10] has schematically summarized the evolution of clusters in Nafion as water content is increased. With increasing water content, the ionic clusters swell, ultimately leading to the formation of cylindrical channels of solvent. As more solvent is absorbed, a sparser network, held together by a framework of hydrophobic chains, is created, which eventually organizes into cylindrical micelles.

In all ionomeric PEMs, the proton transfer depends on obvious factors such as the number of available acid groups and their ability to dissociate in water to create protons. Recently, however, it has become apparent that the properties of the backbone of an ionomer, such as persistence length and its interaction with the solvent, affects supermolecular structure and consequently transport properties.[10,11] The present work is directed at the study of proton transport in a new class of ionomers, accompanied by a structural study of one of these materials.

Work in our laboratories has recently focused on the study of sulfonated styrene/ethylene−butylene /styrene (S-SEBS) triblock copolymer (Figure 1b) as a PEM for use in hydrogen fuel cells.[7,13−15] This material is particularly interesting because of the structural differences between this material and the widely studied perfluorinated sulfonic acid (e.g., Nafion-like) materials.[12,16−22] The differences are manifested in both the chemical composition of the backbone (hydrocarbon vs fluorocarbon), which affects the association characteristics of the polymer chains in an aqueous environment, and the nature of the sulfonate group; that is, S-SEBS bears a phenylsulfonic acid as opposed to the more acidic fluorosulfonic acid found in Nafion.[22] A recent study[14] has compared water uptake, swelling, ^{1}H pulsed gradient spin echo nuclear magnetic resonance (NMR), and variable temperature and pressure/complex impedance/electrical conductivity data on a S-SEBS triblock polymer compared with Nafion. The data suggest significant, systemic differences between these two materials below 10 wt % water. At high water content, the properties of S-SEBS are similar to those for Nafion, proton transport being similar to that in bulk water. For low water contents, however, the conductivity characteristics of the materials diverge. For example, at low water content S-SEBS, the variation of the conductivity with temperature follows Arrhenius behavior while that for Nafion does not.

[†] Dais Analytic Corporation.
[‡] U.S. Naval Academy.
[§] Clemson University.
[⊥] Department of Chemical Engineering, Virginia Commonwealth University.
[#] Department of Medicinal Chemistry, Virginia Commonwealth University.
* Authors for correspondence.

10.1021/ma020251n CCC: $22.00
Published on Web 06/21/2002

a Nafion, n=6.5, x=1

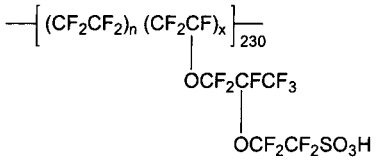

b S-SEBS

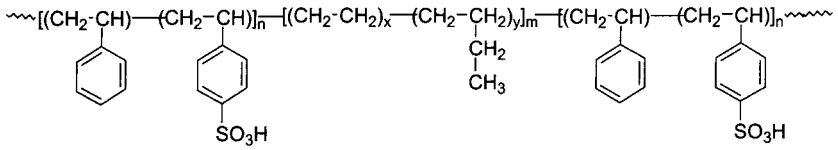

c SE Series

Structure of partially sulfonated styrene-ethylene interpolymer (S-SE), x = 9, 2.5, and 1.2 for S-SE1, S-SE2, and S-SE3 respectively.

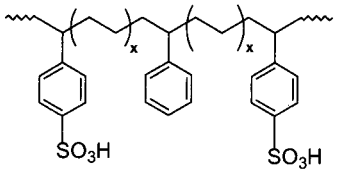

Figure 1. (a) Nafion, $n = 6.5$, $x = 1$. (b) S-SEBS. (c) SE series. Structure of partially sulfonated styrene−ethylene interpolymer (S-SE); $x = 9$, 2.5, and 1.2 for S-SE1, S-SE2, and S-SE3, respectively.

This and many of the differences in the transport properties of ionomers cannot be simply attributed to the number of available ionic species in the system. It is therefore of interest to correlate the transport properties of a PEM with specific chemical and structural features of the polymers themselves. The present study concentrates on comparing S-SEBS with a corresponding random copolymer with the intent of establishing the effects of the molecular architecture on the transport characteristics of the membrane. The advent of a new class of styrene−ethylene (SE) pseudo-random copolymers [23,24] ("interpolymers") developed by Dow Chemical offers an opportunity to probe the effect of composition on electrical and physical properties of sulfonated styrene derivatives (Figure 1c). The comparison between the different materials is indirect with respect to S-SEBS in that the center block of SEBS is hydrogenated poly(butadiene) rather than poly(ethylene), and as such, the former has an irregular structure with a mixture of saturated 1,2- and 1,4-units. In addition, the microphase separation found in S-SEBS that is characteristic of block copolymers is not expected with sulfonated SE (S-SE) polymers, rather, a smaller microdomain morphology associated with aggregation of polar sulfonated styrene units that is perhaps more reminiscent of Nafion. Finally, in S-SEBS, sulfonated styrene units will likely be adjacent to each other as the result of relatively high sulfonation (55 mol %) of the PS homopolymer block. The Dow SE materials are unique in that the metallocene active centers of the catalysts employed in polymerization do not allow multiple styrene additions, and thus each styrene repeat unit is flanked by at least one ethylene repeat unit.[24]

Experimental Section

Sample Preparation. Samples of styrene−ethylene (SE) copolymer were obtained from Dow Chemical with styrene contents ranging from 20 to 75 wt % and were sulfonated by the Dais Analytic Corp. Films ca. 60−80 μm thick were cast from 1-propanol and slowly dried overnight. Films of S-SEBS were prepared at Dais-Analytic. Sulfonation levels were determined by titration of predried membranes against standardized base.

Conductivity Measurements. A film of Nafion 117 was obtained from Aldrich Chemical. Conductivities were determined for membranes immersed in distilled, deionized water at Dais Analytic by the method of Zawodzinski et al.[25] using a Solartron model 1260 frequency response analyzer. Experiments on the dependence of humidity on conductivity were conducted at the U.S. Naval Academy using gold electrodes sputtered onto the ends of the samples. The samples were placed in a chamber where the relative humidity was controlled by an ETS model 514 automatic humidity controller using an ETS 5612C ultrasonic humidification system. All electrical measurements were carried out along the plane of the samples using the same geometry as that used previously for fluorocarbon-based materials.[21] While the samples remained in the chamber, the audio frequency complex impedance of the samples, $Z^* = Z' - jZ''$, was measured using a CGA-83 capacitance bridge, a Hewlett-Packard 4194A impedance/gain-phase analyzer, or a 1255 Solartron high-frequency response analyzer connected to a Solartron 1296 dielectric interface.

Structural Studies. Small- and wide-angle X-ray scattering (SAXS, WAXS) and small-angle neutron scattering (SANS) measurements were carried out on dry and swollen films. Dry films were obtained by holding as-received films in a vacuum oven at room temperature overnight. Wet samples have been prepared by soaking the polymer film in D_2O for ~4 h prior to measurements to increase scattering contrast for the neutron experiment. Excess water was drained. The neutron measurements were carried out at NIST on NG3 SANS at 13 and 3 m, at $\lambda = 6$ Å covering a q range from 0.0015 to 0.06 Å^{-1}, where q is the momentum transfer vector defined as $4\pi \sin\theta/\lambda$. Here θ is the incident angle and λ is the neutron wavelength. X-ray studies were carried out on a Sintag XDS200 powder diffractometer (Cu Kα, $\lambda = 1.54$ Å; SAXS 40 kV, 20 mA; WAXS

Table 1. Conductivity and Water Uptake Data for Three S-SE Samples, S-SEBS, and Nafion

sample	wt % styrene	mol % styrene	ethylene/ styrene[c]	mol % sulfonation	equiv wt	conductivity (S/cm)[b]	% water uptake
S-SE-1	30.0	10.3	8.7	45.2	847	0.002	140
S-SE-2	61.0	29.6	2.4	38.6	522	0.11	420
S-SE-3	75.0	44.7	1.2	36.0	465	0.09	580
S-SEBS	29.0	18.0		55.0	270[a]	0.085	400
Nafion 117					1100	0.079	80

[a] For 55 mol % sulfonated styrene domains; does not consider 70 wt % ethylene/butylene component. [b] Measured at full hydration (after immersion in water for at least 15 min). [c] Ethylene/styrene ratio calculated as mol % ethylene/mol % styrene.

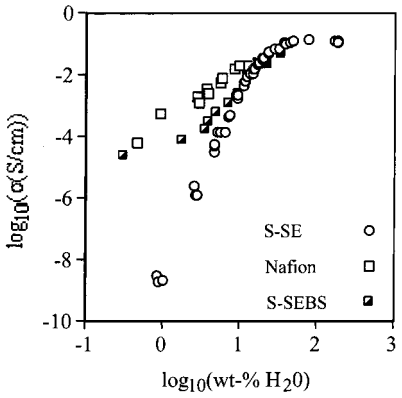

Figure 2. Water content in wt % vs relative humidity at room temperature for S-SE-2 (open circles). The values for Nafion 117 are represented by the open squares; the half-filled squares are the values for S-SEBS.

40 kV, 30 mA). The beam had a rectangular shape (20 mm × 0.8 mm; width at half-maximum). The experiments were carried out in a reflection mode, covering a q range up to 2.8 $Å^{-1}$.

Results and Discussion

Table 1 summarizes data for conductivity at full hydration (water immersion) as a function of copolymer composition and sulfonation level for several SE materials, a sulfonated SEBS triblock polymer, and Nafion. Two sulfonated SE copolymers (S-SE-2 and S-SE-3) exhibit very high conductivities when allowed to swell in water. The conductivities are comparable to those of Nafion and S-SEBS triblock polymer. The particularly high conductivity (ca. 0.1 S/cm) of the 60 wt % styrene/ 40 mol % sulfonation sample (S-SE-2) suggests the presence of a continuous, proton-conducting phase and prompted additional study.

Figure 2 shows data for the conductivity of S-SE-2 as a function of water content and compares recent data for Nafion and S-SEBS.[3] The high conductivity of the SE sample is evident at the highest hydration levels along with a more precipitous drop in conductivity with decreasing humidity compared with the cases of Nafion and S-SEBS. We will discuss this trend more fully after introducing the structural characteristics of a representative polymer from this group, S-SE2, in dry and fully hydrated states.

Films of S-SE2 have been studied by X-ray and neutron scattering. Figure 3 displays the X-ray patterns, and Figure 4 introduces the neutron results for dry and fully hydrated samples, together covering a large range of periodicities. The X-ray pattern of a dry film consists of broad lines at ~34 and 4.6 Å. Sharper, crystalline lines are observed at 9.3, 4.6, and 3.1 Å. These lines correspond to residues of talc ($Mg_3Si_4O_{10}(OH)_2$) used to minimize adhesion of tacky particles of raw SE polymer. While the lines may appear rather intense, when

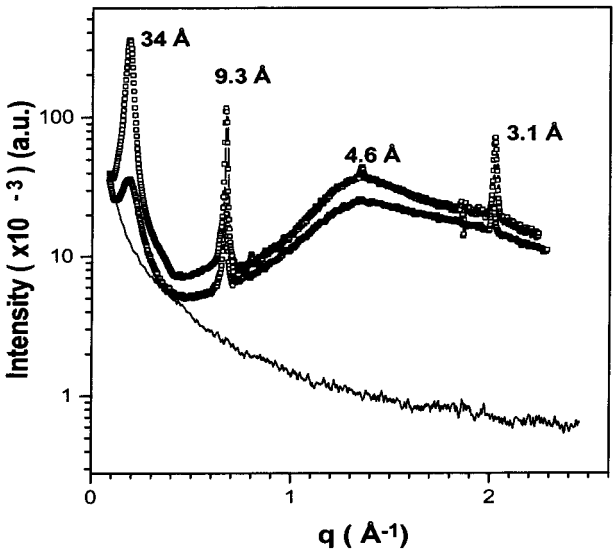

Figure 3. X-ray pattern of S-SE2; dry (open squares) and wet (circles) samples were measured at room temperature. The solid line at the bottom corresponds to the background. Several instrumental configurations have been used to cover the entire q range, and the intensity is normalized accordingly.

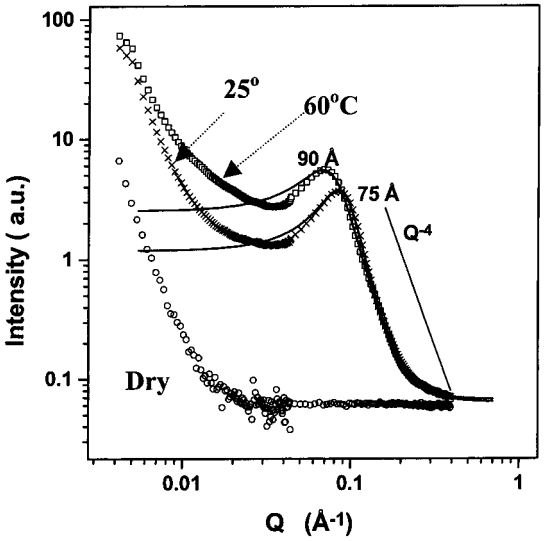

Figure 4. Small-angle neutron scattering of S-SE2, dry and fully hydrated films at 25 and 60 °C. The q^{-4} line is a calculated guideline. The solid lines connecting the experimental points correspond to fitting of the experimental results to a Teubner−Strey bicontinuous model.

normalized to the absorption coefficient and to the scattering cross section of the inorganic and organic components, as well as the degree of crystallinity, it becomes clear that only a minute fraction of the mineral is left. Since its crystallographic structure is well established, it was further utilized as a calibration reference.

The width of the lines 34 and 4.6 Å suggests that they correspond to periodically occurring structural features of amorphous polymers. The positions of these lines are not sufficient to determine their origin. The peak at 4.6 Å is in the range where both aliphatic chains and substituted aromatic moieties are observed. The line at 34 Å is in the range for interdomain correlation. This line may correspond to correlation between either hydrophobic or ionic clusters. However, further information is required to assign these lines. Upon swelling of the membrane, the positions of the 34 and 4.6 Å lines do not change (in q space). However, the intensity of the 34 Å line increases dramatically while the 4.6 Å line hardly changes. This suggests that the 4.6 Å line corresponds to a repeating distance within the hydrocarbon domains, which are not accessible to the polar solvent. The width of this line comprises the q range characteristic of interacting aliphatic and aromatic components. Since this line is not affected by the presence of water, we assign it to the intermolecular distance within the hydrophobic region. We cannot, however, distinguish between the aliphatic chains and the aromatic groups.

The line at 34 Å increases in intensity as water is added but does not shift in q space. The increase in intensity may be a result of increasing scattering contrast, increasing order or an increasing number of scattering units. The change in intensity with swelling without changing dimensions suggests that the peak is related to a hydrophobic periodicity. The most natural assignment would be the interdomain distance between the hydrophobic regions. However, with increasing water content, the hydrophobic interdomain distance is expected to increase. In the present system, we have no direct evidence for either an increase in the number of scattering particles or an increase in ordering with swelling. Therefore, it is suggested that this increase is due to an increase in contrast when D_2O is added and to a sharpening of domain boundaries. The value remains fixed as the system swells, which suggests that this line is associated with the size of hydrophobic domains, which are, as noted above, inaccessible to the solvent. When water is added, a better segregation between hydrophilic and hydrophobic regions is achieved, thus releasing stress in the system and allowing more defined aggregates.

The SANS, which can probe larger dimensions, has been employed to both dry and wet samples of S-SE-2. While the X-ray pattern consists of two distinct peaks, the SANS pattern of the dry sample exhibits no signal at the measured q range (which is complementary to the X-ray data). Upon hydration, a distinct peak at the intermediate q range and a further diffuse signal at lower q are observed. The signal at very low q is characteristic of a very large object or a network with large correlations.[26] This characteristic signal appears very close to the main beam and is difficult to resolve; thus, we could not obtain a quantitative fit. On the basis of the observation that the membrane does not dissociate when saturated with water, we suggest that the origin of this signal is a sparse hydrophobic network supporting the film even at very high hydration level despite the absence of physical cross-links. The peaks at $q = 0.084$ and 0.07 Å^{-1} appear with hydration of the sample and indicate a new periodicity in addition to those observed by SAXS. The correlation length associated with this peak is given by $l = 2\pi/q_{max}$, values for which are given in Table 2. As the sample swells, segregation into aqueous and hydrocarbon domains takes place, the sulfonate groups defining the interfaces.

Table 2. Fit Parameters for the Teubner and Strey Bicontinuous Model

temp (°C)	d (Å)	ξ (Å)	d/ξ	l
25	71	38	1.87	75
60	85	35	2.42	90

Porod's law[26] relates the intensity at the high q range of a scattering pattern and includes the contribution of local interfaces of the sample. The intensity, I, is given by

$$I = (\Delta\rho)^2 \frac{2\pi}{q^4} S \qquad (1)$$

where $\Delta\rho$ is the scattering contrast and S is the total internal surface. This relationship will hold for particles and nonparticulate systems, provided there is a well-defined internal surface.[26] The SANS data of the swollen membranes show a broad peak that exhibits a characteristic q^{-4} dependence at high q values, suggestive of the formation of a well-defined interface upon hydration. While a sharp interface is present and a rather large correlation length has been established, further experiments are needed in order to resolve the shape of these domains. For many ionomers, an "ionomer peak" is observed, and the corresponding ionomer cluster is found to be spherical or elliptical, based on the counterion.[6,9] Models based on closed domains (such as ionic clusters, hydrophobic domains, etc.) yield very limited agreement with experimental data. At best, a reasonable fit is obtained for a very narrow q range around q_{max}, and the fit diverges appreciably at high and low q. Following the model recently suggested by several groups,[9,10] the present data have been analyzed in terms of a bicontinuous distribution of hydrophilic and hydrophobic domains.

A single broad peak with a q^{-4} decay at large q indicates a sharp interface as is often observed in polymeric micelles in poor solvents and in bicontinuous phases.[27] In the system under discussion, the possibility of a micellar structure is tentatively excluded since the film does not dissolve under the conditions studied. One can thus consider a model of a bicontinuous phase, where water channels are intertwined with a partial mesh of hydrocarbon chains and in which the sulfonate groups constitute the interface. The data at the intermediate q range were fitted to the Teubner and Strey bicontinuous model.[27] The Teubner and Strey model is widely used to describe this two-component structure when the particle shape is not well-defined. The model is based on Ginzburg−Landau theory, describing two characteristic length scales: d and ξ, where d represents an interdomain distance and ξ is a correlation length that is a measure of the dispersion of d. In the swollen membrane, d is the average distance between water−water domains or polymer−polymer domains. The fit parameters are listed in Table 2. As pointed out previously, the data at low q indicate the presence of a hydrophobic mesh with very large dimensions. Even though the data extend over a very large q range, the values of q are not low enough to completely characterize that mesh.

The fitted domain size, d, is close to the interaction length calculated from the q_{max}, and the value of ξ is rather close to one of the correlation lengths, ~34 Å,

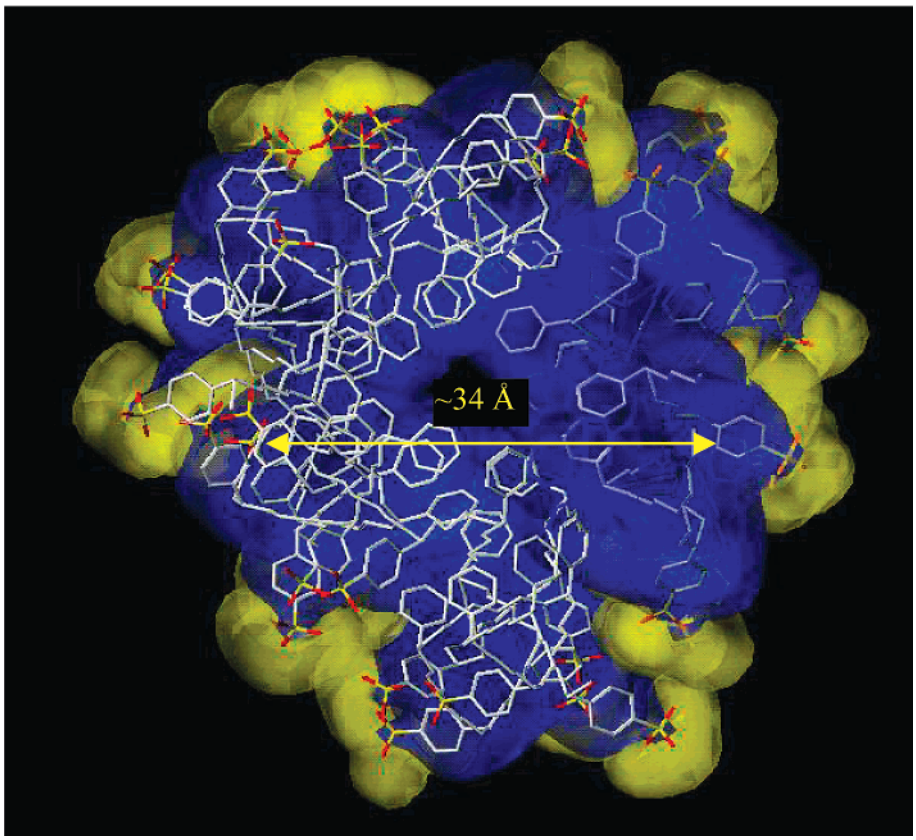

Figure 5. Visualization of a hydrophobic cluster. SYBYL version 6.7 (Tripos) and HINT (Hydropathic INTeractions) computational modeling software[28] have been used to minimize the configurational energy of individual S-SE2 chains of 80 carbons each. The HINT program was employed to create hydrophobic/hydrophilic contour maps for each of the chains, which were subsequently assembled to create the image allowing 34 Å for the hydrophobic domains. HINT depiction of six S-SE chains showing hydrophobic regions (blue) with peripheral hydrophilic sulfonates (yellow) end-on view.

obtained in the X-ray pattern for the dry and wet films. Thus, ξ may correspond to the average width of a hydrophobic pocket. Since ξ is a measure of the dispersion of d, the ratio of d/ξ is inversely proportional to the order of the domains. As the temperature increases, d/ξ increases, indicating the disordering of the domains with increasing temperature. This may represent the onset of the dissolution of the membrane.

The scattering data have been obtained for two extremes, dry and fully wet films. While the scattering patterns consist of very few lines, they clearly show that, with swelling, the intermediate and high q data do not change in q, and a new feature appears at low q. The available models for ionomers did not yield a reasonable fit. However, the bicontinuous network recently suggested by Gebel[10] and Kreuer[11] was found to be consistent with both scattering and transport[14] measurements.

On the basis of the dimensions obtained by scattering, a strictly qualitative model has been constructed. We have attempted to visualize a hydrophobic cluster using SYBYL version 6.7 (Tripos) and HINT (Hydropathic INTeractions) computational modeling software.[28] Figure 5 was generated using six discrete, separately energy-optimized S-SE2 chains. The HINT program was employed to create hydrophobic/hydrophilic contour maps for each of the chains, which were subsequently assembled to create the image. In Figure 5, hydrophobic regions appear in blue, and hydrophilic regions appear in yellow. The chains were organized to place sulfonates on the periphery of the cluster, as would be expected upon hydration. While we cannot simulate the entire hydrogel including the solvent, this model is fully consistent with the bicontinuous nature of the hydrated phase as observed from SANS. The model is also consistent with the results presented for different ionomers including Nafion and sulfonated poly(ether ketone)s.[11,12]

We conclude with a brief discussion of the conductivity data in Figure 2 in light of the structural information discussed above, beginning with a comparison of Nafion and S-SE2. The conductivity, σ, of a material with a single type of charge carrier is given by

$$\sigma = ne\mu \tag{2}$$

where n is the number of carriers per unit volume, e is the charge (the magnitude of the charge for hydrated protons can be ignored here), and μ is the mobility (typical units of $cm^2/V{\cdot}s$). The key quantity is the product $n\mu$, which for a material such as water-swollen Nafion is high since the conductivity is high. At low water content, the conductivity of S-SE2 is several orders of magnitude lower than that of Nafion, and it is tempting to suggest that this is the result of the higher basicity of phenylsulfonate anions, which limit hydrated proton mobility. However, a simliar argument should hold for S-SEBS, yet its conductivity tracks that of Nafion much more closely. We suggest that in S-SEBS the natural microphase separation of the block copolymer affords interconnecting sulfonated styrene domains and thereby inherently good mobility, the role of water being principally to generate carriers by ionization of sulfonic acids. In the case of S-SE, we believe that the

creation of a bicontinuous domain structure requires water, and hence water plays the dual role of creating conducting pathways as well as carriers. It is reasonable to suggest that some of the sulfonates are buried in hydrophobic clusters (Figure 5) in the absence of water, with reorganization occurring upon hydration and subsequent percolation to place sulfonates at the periphery to form continuous hydrophilic channels. As noted earlier, the reorganization and enhanced segregation of polar and nonpolar components might account for the increase in the intensity of the 34 Å X-ray peak upon hydration.

Conclusions

A new class of proton-conducting polymers has been identified on the basis of partially sulfonated, ethylene−styrene pseudo-random copolymers. At full hydration, conductivities as high as 0.1 S/cm are routinely observed, and evidence of a bicontinuous phase has been observed by SANS. These data lead us to propose a bicontinuous phase model to account for the high conductivity and hydrogel-like properties. We believe that these materials are promising candidates for low-temperature proton exchange membrane-based fuel cells and related applications.

Acknowledgment. We thank Alastair Hill of the Dow Chemical Company for samples of styrene−ethylene copolymers and Drs. Boualem Hammouda and Steve Klein (NIST) for their kind assistance on NG3 SANS30m and fruitful discussions. This work was supported in part by a grant from the U.S. Office of Naval Research (to J.J.F.) and the NSF Partnerships for Innovation Program (subcontract from Virginia Tech to G.E.W.).

References and Notes

(1) Gottesfeld, S.; Zawodzinski, T. A. In *Advances in Electrochemical Science and Engineering*; Alkire, R. C., Geridches, H., Kdb, D. M., Tobias, C. W., Eds.; Wiley-VCH: New York, 1997; Vol. 5, p 195.
(2) Mokrini, A.; Acosta, J. L. *J. Appl. Polym. Sci.* **2002**, *83*, 367.
(3) (a) Moffitt, M.; Eisenberg, A. *Macromolecules* **1997**, *30*, 4363. (b) Shin, K.; Rafailovich, M. H.; Sokolov, J.; Gersappe, D.; Kim, M. W.; Satija, S. K.; Nguyen, D.; Xu, D.; Yang, N.-L.; Eisenberg, A. *Langmuir* **2002**, *17*, 6675.
(4) Moor, R. B., III; Martin, C. R. *Macromolecules* **1989**, *22*, 3594.
(5) Hill, T. A.; Jiao, X.; Martin, C. W.; DesMarteau, D. D.; Perahia, D. In *Dynamics of Small Confined Systems IV*; Drake, J. M., et al., Eds.; MRS Publishing: New York, 1999; p 189.
(6) Sauer, B. B.; Mclean, S. R. *Macromolecules* **2000**, *33*, 7939.
(7) Serpico, J. M.; Ehrenberg, S. G.; Fontanella, J. J.; McGrady, K. A.; Perahia, D.; Jiao, X.; Sanders, E. H.; Wallen, T. M.; Wnek, G. E. *PMSE Prepr.*, in press.
(8) Kreuer, K.-D. *Chem. Mater.* **1996**, *8*, 610.
(9) Kirkmeyer, B. P.; Weiss, R. A.; Winey, K. I. *J. Polym. Sci., Part B: Polym. Phys.* **2001**, *39*, 477.
(10) (a) Gebel, G.; Lambard, J. *Macromolecules* **1997**, *30*, 7914. (b) Gebel, G. *Polymer* **2000**, *41*, 5829.
(11) Kreuer, K. D. *J. Membr. Sci.* **2001**, *185*, 29.
(12) Wnek, G. E.; Rider, J. N.; Serpico, J. M.; Einset, A. G.; Ehrenberg S. G.;. Raboin, L. *Proc. First International Symposium on Proton Conducting Membrane Fuel Cells; Electrochem. Soc. Proc.* **1995**, *247*, 95.
(13) Wnek, G. E.; Sheikh-Ali, B. M.; Serpico, J. M.; Ehrenberg, S. G.; Tangredi, T. N.; Karuppaiah, C.; Ye, Y. *Polym. Prepr.* **1998**, *39*, 54.
(14) Edmondson, C. A.; Fontanella, J. J.; Chung, S. H.; Greenbaum, S. G.; Wnek, G. E. *Electrochim. Acta* **2001**, *46*, 1623.
(15) Wintersgill, M. C.; Fontanella, J. J. *Electrochim. Acta* **1998**, *43*, 1533.
(16) Fontanella, J. J.; Wintersgill, M. C.; Chen, R. S.; Wu, Y.; Greenbaum, S. G. *Electrochim. Acta* **1995**, *40*, 2321.
(17) Fontanella, J. J.; McLin, M. G.; Wintersgill, M. C. *J. Polym. Sci., Part B: Polym. Phys.* **1994**, *32*, 501.
(18) Chen, R. S.; Jayakody, J. P.; Greenbaum, S. G.; Pak, Y. S.; Xu, G.; McLin, M. G.; Fontanella, J. J. *J. Electrochem. Soc.* **1993**, *140*, 889.
(19) Zawodzinski, T. A., Jr.; Derouin, C.; Radzinski, S.; Sherman, R. J.; Smith, V. T.; Springer, T. E.; Gottesfeld, S. *J. Electrochem. Soc.* **1993**, *140*, 1041.
(20) Edmondson, C. A.; Stallworth, P. E.; Chapman, M. E.; Fontanella, J. J.; Wintersgill, M. C.; Chung, S. H.; Greenbaum, S. G. *Solid State Ionics* **2000**, *135*, 419.
(21) Fontanella, J. J.; Edmondson, C. A.; Wintersgill, M. C.; Wu, Y.; Greenbaum, S. G. *Macromolecules* **1996**, *29*, 4944.
(22) The pK_a for Nafion has been estimated to be ca. −6; that of a typical phenyl sulfonate is ca. −1. See ref 11, p 32.
(23) Chen, H.; Guest, M. J.; Chum, S.; Hiltner, A.; Baer, E. *J. Appl. Polym. Sci.* **1998**, *70*, 109.
(24) (a) Cheung, Y. W.; Guest, M. J. *ANTEC '96 SPE Conf. Proc.* **1996**, 1634. (b) Swogger, K. W.; Chum, S. P. In *Metcon '97 "Polymers in Transition" Conference Proceedings*, 1997. (c) Mudrich, S. F.; Cheung, Y. W.; Guest, M. J. In *Antec'97 SPE Conference Proceedings*, 1997; pp 1783−1787.
(25) Zawodzinski, T. A., Jr.; Neeman, M.; Sillerud, L. O.; Gottesfeld, S. *J. Phys. Chem.* **1991**, *95*, 6040.
(26) Glatter; O.; Kratky, O. In *Small-Angle X-ray Scattering*; Academic Press: London, 1982.
(27) Teubner, M.; Strey, R. *J. Chem. Phys.* **1987**, *87*, 3195.
(28) Burnett, J. C.; Kellogg, G. E.; Abraham, D. J. *Biochemistry* **2000**, *39*, 1622.

MA020251N